Dual-Cross-Polarized Antenna Decoupling for 43 GHz Planar Massive MIMO in Full Duplex Single Channel Communications

Muhsin[1]

Faculty of Electrical Engineering
Institut Teknologi Telkom Surabaya
Surabaya, Indonesia

Rina Pudji Astuti[2]

School of Electrical Engineering
Telkom University
Bandung, Indonesia

Abstract—**Massive Multiple Input Multiple Output (MIMO) and Full Duplex Single Channel (FDSC) at mm-Wave are key technology of future advanced wireless communications. Self-interference is the main problem in this technique because big number of antennas. This paper proposes dual-cross-polarized configuration to reduce self-interference between antennas. We conduct some computer simulations to design the antenna and to verify self-interference effect of the designed antenna. Computer simulation shows that the proposed design has lower Envelope Correlation Coefficient (ECC). This result is achieved because dual-cross-polarized technique can reduce coupling between antennas. We found that bit-error-rate (BER) performances of the proposed antenna is better than single polarized antenna indicating that the designed antenna is well design to reduce self-interference effect between antennas.**

Keywords—*Massive MIMO; dual polarized; mm-Wave; coupling; self-interference; full duplex single channel*

I. INTRODUCTION

FDSC on massive MIMO at mm-Wave offers better performance compared to conventional communications using FDD or TDD on Single Input Single Output (SISO). Massive MIMO provides high degree of diversity [1]–[3] and FDSC simultaneously which transmit and receive signals in same frequency and time [4]–[8]. Combination of FDSC and massive MIMO is excepted having benefits from both techniques.

Self-interference is the main problem of implementing FDSC on massive MIMO. It caused by duplexer's leakage and coupling matrix between antennas. Coupling matrix between antennas become greater with increasing number of antennas. Low coupling is needed to reduce amount of self-interference. Dual-cross-polarized antenna [9], [10] and sectoral antenna [11] are two main methods to achieve low coupling.

Sectoring antenna is potentially the most suitable configuration in base station. Low coupling is achieved by make low intersection between antennas' radiation pattern by sectoring antenna which has high gain. Each sector only served by partial number of antennas, there antennas usually formed as array to achieve high gain. Previous research in [11] use this method for dual band massive MIMO antenna at 28 and 38 GHz.

Planar antenna is the most common antenna for high frequency application. Dual polarized method can be easily applied in planar antenna to minimize coupling effect. It has been shown in [10], [12] that dual polarized in planar configuration can reduce coupling and improve isolation between antennas. These research has been done in low number of antennas and lower frequency. More massive number of antennas in mm-Wave has been evaluated in [9], [13]. Another technique to improve antenna isolation using absorptive shielding has been proposed in [14]. This technique is not suitable for massive MIMO becuase of high number of antenna.

This paper proposed dual polarized antenna decoupling for FDSC evaluated at 43 GHz. This technique can reduce self-interference by reducing coupling between antennas. 4×4 planar array MIMO at 43 GHz is used as basic model with single polarized and dual polarized configuration. These antennas are tested in simulation system considering self-interference with and without S-parameter matrix based self-interference cancellation.

Antenna design is presented in Section II starting from single element to full 16 elements MIMO antenna with both single polarized and dual polarized configurations. Simulation model of self-interference is explained in Section III. Antennas are evaluated by ECC and BER performance in Section IV and V, respectively. Finally, conclusion is pretested in Section VI.

II. ANTENNA DESIGN

Basic model of antenna design in microstrip planar antenna with circular disk proximity coupled. This model is chosen due to its flexibility. Both single polarized and dual polarized model are extended from this basic model.

Design process is started with single antenna model using basic model. This basic single antenna then extended into single cluster composed from four single antennas. Finally, final antenna for both single polarized and dual polarized configurations are formed by duplicating single cluster of antenna model. This clustering method is chosen to simplify design process.

A. Single Antenna Design

Single antenna is formed as basic model of MIMO array. Stepping of design is started by this single antenna model. Single antenna is modeled and optimized in order to get its best performance. The performance can be measured by return loss because antenna works at certain value of return loss.
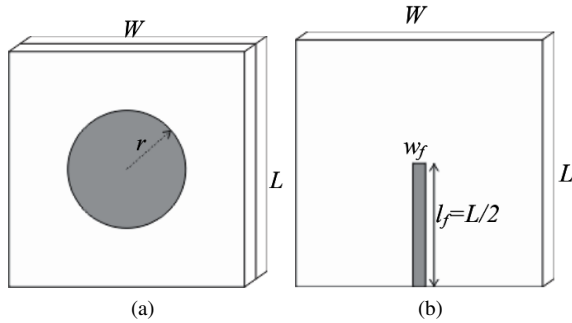
Fig. 1. Geometry of circular disk proximity coupled antenna: (a) top layer, (b) middle layer
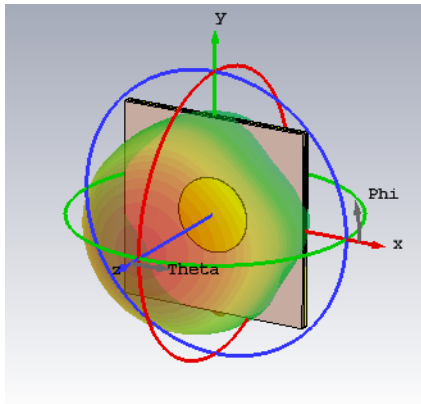

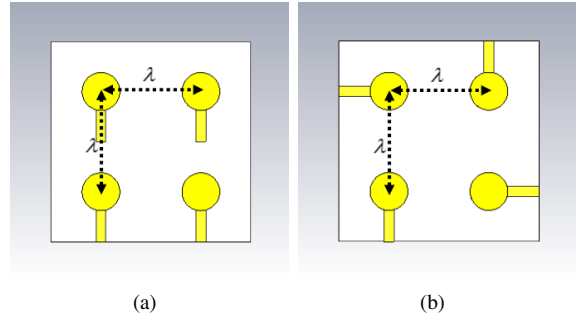Fig. 2. Radiation pattern of single antenna.

Fig. 3. Single cluster of the antenna: (a) single polarized MIMO antenna, (b) dual polarized MIMO antenna.

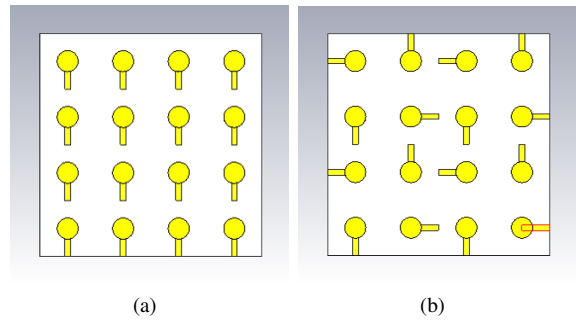Fig. 4. Final model of the antenna: (a) single polarized MIMO antenna, (b) dual polarized MIMO antenna.

Each single antenna is designed as circular disk proximity coupled antenna as shown in Figs. 1(a) and 1(b). Rogers RT-5880 with $h = 0.127$ mm is used as substrate's material with permittivity $\epsilon_r = 2.2$.

Basic formula in [15] has simplified as

$$r = \frac{F}{\sqrt{1 + \frac{2h}{\pi \epsilon_r F} \left[\ln \left(\frac{\pi F}{2h} + 1.7726 \right) \right]}} \qquad (1)$$

with

$$F = \frac{8.791 \times 10^9}{f \sqrt{\epsilon_r}}, \qquad (2)$$

where h is depth or height of substrate in cm, f is antenna's resonance frequency, and ϵ_r is substrate's relative permittivity.

Antenna is design and optimized at 43 GHz resonant frequency and 50 Ω reference impedance. The result is antenna's width $W = L = \lambda = 6.98$ mm, length of feed $l_f = W/2 = 3,49$ mm, width of feed $w_f = 0.70$ mm, and disk radius $r = 1.30$ mm.

Single antenna model has unidirectional radiation pattern with 7.456 dBi gain with total efficiency of -0.1933 dB as shown in Fig. 2. Formed planar massive MIMO antenna by using this single antenna is also unidirectional. This configuration is suitable for single sector sectoral massive MIMO base station as in [11].

B. Clustering

Clustering method is chosen in order to simplify the design process. A single cluster of each configuration are shown in Fig. 3 using a wavelength spacing between antennas' center horizontally and vertically. Polarization variation is set by different direction of feeding.

Single antenna is set as basis of single cluster using dimensional parameter from Section II-A. This model then optimized to get the best performance in a single cluster. It assured antenna's performance in smaller number of antennas before final model is formed. There is an assumption that significant change only happened in 1 to 4 elements expansion.

C. Final Model of The Antenna

Different feeding is applied to each configuration to get different polarization characteristic. Single polarized antenna is fed with same direction as shown in Fig. 4(a). Dual polarized antenna is fed with cross direction as shown in Fig. 4(b). It is made by extend single cluster to form full 16 elements MIMO antenna.

Designed antenna has 8 sectors in total shown in Fig. 5(a). Each sector has total 16 antennas with 4×4 planar configuration. Antennas are numbered for each single element from left-top to bottom right. This numbering is used to identify each single antenna. Antennas numbering is shown in Fig. 5(b). Clustering is applied for 4 near antennas, for example antenna 1, 2, 5, and 6 are in the same cluster. There are 4 clusters composed massive MIMO antenna for each configuration.
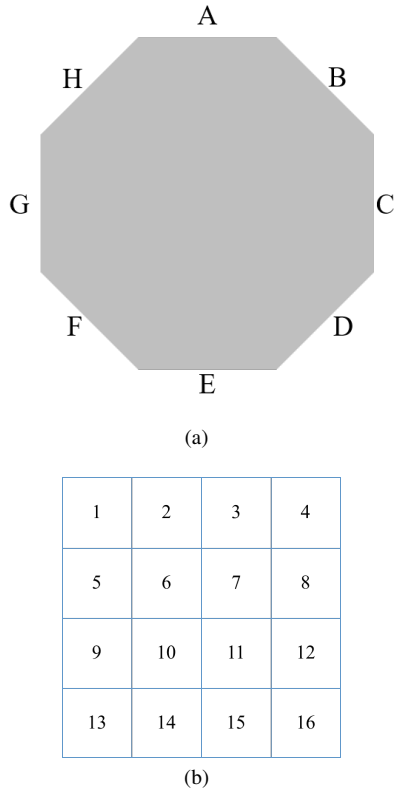
(a)

(b)

Fig. 5. Antenna's sectoring and numbering: (a) sectoring, (b) numbering.

III. SIMULATION MODEL

There are three parts explained in this section. First part is self-interference model. Quasi-Orthogonal Space Time Block Code (QOSTBC) for full rate massive MIMO is explained in second part of this section. Last part explains self-interference management for massive MIMO FDSC.

A. Self-Interference

Self-Interference is the main problem in FDSC as described in [4]–[8], [16]. Self-interference is interference part caused by the node itself. In this case, self-interference caused by duplexer's leakage and coupling between antennas. It can be modeled as

$$\mathbf{y} = \mathbf{H}\mathbf{x} + \mathbf{S}\mathbf{w} + \mathbf{L}_I\mathbf{w} + \mathbf{n}_0 \qquad (3)$$

where $\mathbf{y}$ is received signal, $\mathbf{x}$ is transmitted information signal, $\mathbf{w}$ is transmitted self-interference signal, and $\mathbf{n}_0$ is Additive White Gaussian Noise (AWGN). This model is shown in Fig. 6. Self-interference is caused by $\mathbf{S}$ and $\mathbf{L}_I$ with

$$\mathbf{S} = \begin{pmatrix} s_{11} & s_{12} & \cdots & s_{1N} \\ s_{21} & s_{22} & \cdots & s_{2N} \\ \vdots & \vdots & \ddots & \vdots \\ s_{N1} & s_{N2} & \cdots & s_{NN} \end{pmatrix} \qquad (4)$$

and

$$\mathbf{L}_I = \begin{pmatrix} L_1 & 0 & 0 & \cdots & 0 \\ 0 & L_2 & 0 & \cdots & 0 \\ 0 & 0 & L_3 & \cdots & 0 \\ \vdots & \vdots & \vdots & \ddots & \vdots \\ 0 & 0 & 0 & \cdots & L_N \end{pmatrix} \qquad (5)$$
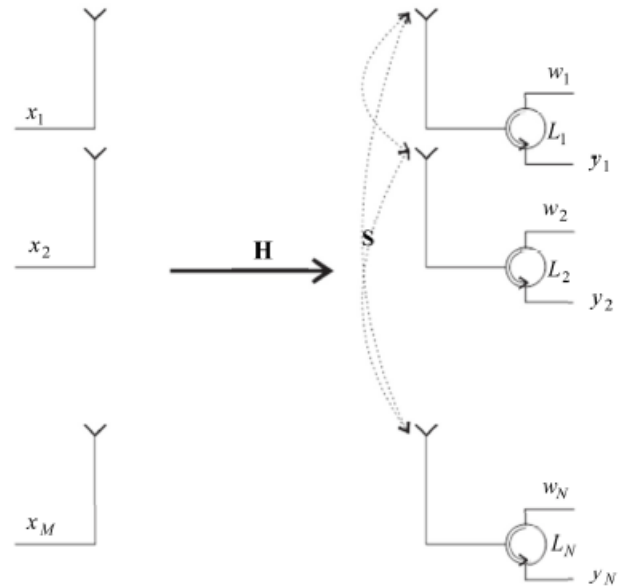

Fig. 6. Model of self-interference by other antennas and duplexer's leakage.

where each element of $\mathbf{S}$ represents coupling between antennas and diagonal element of $\mathbf{L}_I$ represents duplexer's leakage at each antenna. Both of these matrix's ideal values are 0 which means no coupling and no duplexer's leakage.

B. Quasi Orthogonal Space Time Block Code (QOSTBC)

QOSTBC is used as MIMO coding in this research. QOSTBC can achieve full rate characteristics by making quasi or semi orthogonal on its MIMO coding. It brings rate and orthogonality trade-offs by making full rate Space Time Block Code (STBC) allowing certain acceptable orthogonality value.

There are two types of QOSTBC proposed in [17], [18]. Extended-Alamouti QOSTBC has pattern of

$$\mathbf{C}_{EA} = \begin{pmatrix} \mathbf{A} & \mathbf{B} \\ -\mathbf{B}^* & \mathbf{A}^* \end{pmatrix} \qquad (6)$$

with each of $\mathbf{A}$ and $\mathbf{B}$ is Alamouti coded signal. If $\mathbf{A}$ is Alamouti coded signal of x_1 and x_2,

$$\mathbf{A} = \begin{pmatrix} x_1 & x_2 \\ -x_2^* & x_1^* \end{pmatrix}. \qquad (7)$$

If $\mathbf{B}$ is Alamouti coded signal of x_3 and x_4,

$$\mathbf{A} = \begin{pmatrix} x_3 & x_4 \\ -x_4^* & x_3^* \end{pmatrix}. \qquad (8)$$

EA-QOSTBC for 4 coded signal by substituting (7) and (8) to (6) is

$$\mathbf{C}_{EA} = \begin{pmatrix} x_1 & x_2 & x_3 & x_4 \\ -x_2^* & x_1^* & -x_4^* & x_3^* \\ -x_3^* & -x_4^* & x_1^* & x_2^* \\ x_4 & -x_3 & -x_2 & x_1 \end{pmatrix}. \qquad (9)$$

Another popular typr of QOSTBC is ABBA QOSBC. In ABBA QOSTBC,

$$\mathbf{C}_{ABBA} = \begin{pmatrix} \mathbf{A} & \mathbf{B} \\ -\mathbf{B} & \mathbf{A} \end{pmatrix}. \qquad (10)$$

ABBA QOSTBC by substituting (7) and (8) to (10) is

$$\mathbf{C}_{ABBA} = \begin{pmatrix} x_1 & x_2 & x_3 & x_4 \\ -x_2^* & x_1^* & -x_4^* & x_3^* \\ x_3 & x_4 & x_1 & x_2 \\ -x_4^* & x_3^* & -x_2^* & x_1^* \end{pmatrix}. \tag{11}$$

These pattern of EA-QOSTBC and ABBA QOSTBC can be repeated until $2^n \times 2^n$ matrix is formed with n is number of coded signals or symbols. In this research, we consider ABBA QOSTBC due to its simplicity.

C. Equivalent Virtual Channel Matrix (EVCM)

EVCM take advantages of mathematical property by transform coded signals into coded channel matrix [18] It can simplify simulation and MIMO decoding process by assuming relatively same response of channel in a single period of coded signals.

Let say there is received signal vector for one receive antenna is

$$\mathbf{r} = \mathbf{C}_x \mathbf{h} + \mathbf{v} \tag{12}$$

with $\mathbf{C}_x$ is coded transmit signal, $\mathbf{h} = \begin{bmatrix} h_1 & h_2 & \cdots & h_{N_C} \end{bmatrix}^T$ is a set of independent channel, and $\mathbf{v} = \begin{bmatrix} v_1 & v_2 & \cdots & v_{N_C} \end{bmatrix}^T$ is equivalent additive noise where N_C is length of STBC in time domain. For two antennas case using Alamouti SBTC,

$$\begin{pmatrix} r_1 \\ r_2 \end{pmatrix} = \begin{pmatrix} x_1 & x_2 \\ -x_2^* & x_1^* \end{pmatrix} \begin{pmatrix} h_1 \\ h_2 \end{pmatrix} + \begin{pmatrix} v_1 \\ v_2 \end{pmatrix} \tag{13}$$

$$\begin{pmatrix} r_1 \\ r_2 \end{pmatrix} = \begin{pmatrix} h_1 x_1 & h_2 x_2 \\ h_2 x_1^* & -h_1 x_2^* \end{pmatrix} + \begin{pmatrix} v_1 \\ v_2 \end{pmatrix}. \tag{14}$$

Conjugating second row of (14),

$$\begin{pmatrix} r_1 \\ r_2 \end{pmatrix} = \begin{pmatrix} h_1 x_1 & h_2 x_2 \\ h_2^* x_1 & -h_1^* x_2 \end{pmatrix} + \begin{pmatrix} v_1 \\ v_2^* \end{pmatrix} \tag{15}$$

$$\begin{pmatrix} r_1 \\ r_2^* \end{pmatrix} = \begin{pmatrix} h_1 & h_2 \\ h_2^* & -h_1^* \end{pmatrix} \begin{pmatrix} x_1 \\ x_2 \end{pmatrix} + \begin{pmatrix} v_1 \\ v_2^* \end{pmatrix} \tag{16}$$

which equivalent with

$$\begin{pmatrix} y_1 \\ y_2 \end{pmatrix} = \begin{pmatrix} h_1 & h_2 \\ h_2^* & -h_1^* \end{pmatrix} \begin{pmatrix} x_1 \\ x_2 \end{pmatrix} + \begin{pmatrix} n_1 \\ n_2 \end{pmatrix} \tag{17}$$

.

D. Self-Interference Management

There are some methods to manage effect of self-interference. In this paper, these methods are categorized into four main methods. All of these methods are focused on reducing or cancelling self-interference in the systems. These four main methods are receiving-transmitting power control, antenna decoupling, isolated duplexer, and cancellation by self-interference cancellation matrix.

Receiving-transmitting power control are focusing on reducing self-interference signal power ratio defined as

$$\alpha_i = \frac{P_{Tx-i}}{P_{Rx-i}} \tag{18}$$

for node, base station, or user i. P_{Tx-i} and P_{Tx-i} are transmitted power and received power on node, base station, or user i. In node i, it is evaluated using (3) by

$$\alpha_i = \frac{\mathrm{pow}(\mathbf{S}\mathbf{w} + \mathbf{L}_I \mathbf{w})}{\mathrm{pow}(\mathbf{H}\mathbf{x})} \tag{19}$$

where $\mathrm{pow}(z)$ represents power of z. Effect of self-interference is decreasing if α can be reduced.

Antenna decoupling are focusing on value of on (3). If this part can be reduced close to zero, receive signal equation become

$$\mathbf{y} = \mathbf{H}\mathbf{x} + \mathbf{L}_I \mathbf{w} + \mathbf{n}_0. \tag{20}$$

If $\mathbf{S}$ is reduced, effect if Sw in (3) also reduced. This decoupling is realized by modifying S-Parameter of the antenna by some antenna design technique.

Isolated duplexer works by using near-perfect duplexer with leakage near to zero. Assuming duplexer's leakage can be eliminated, receive signal equation become

$$\mathbf{y} = \mathbf{H}\mathbf{x} + \mathbf{S}\mathbf{w} + \mathbf{n}_0 \tag{21}$$

which left $\mathbf{S}\mathbf{w}$ as self-interference part. Effect of $\mathbf{L}_I \mathbf{w}$ is reduced if duplexer's leakage is reduced.

Cancellation by self-interference cancellation matrix works by reducing receive signal (3) by

$$\mathbf{SIC} = \mathbf{S}\mathbf{w} + \mathbf{L}_I \mathbf{w}. \tag{22}$$

Assuming $\mathbf{S}$ and $\mathbf{L}_I$ can be predicted, this self-interference cancellation matrix can be formed.

Each of self-interference managements method have its challenge. In this research, we assume linear deviation on antenna decoupling. Received signal is

$$\mathbf{y} = \mathbf{H}\mathbf{x} + \tilde{\mathbf{S}}\mathbf{w} + \mathbf{L}_I \mathbf{w} + \mathbf{n}_0 \tag{23}$$

with deviated scattering parameter

$$\tilde{\mathbf{S}} = \mathbf{S} + k\mathbf{I}. \tag{24}$$

$\mathbf{S}$ is default-mean scattering parameter, k is normally distributed value with zero mean and σ deviation, and $\mathbf{I}$ is identity matrix. Self-interference cancellation matrix is using mean value in (22).

IV. ENVELOPE CORRELATION COEFFICIENT OF ANTENNA MODEL

In this section, both single polarized and dual polarized configuration are evaluated by ECC. This coefficient represents correlation between antennas. ECC can be calculated from antenna's scattering parameter using [19], [20]

$$\rho_{env} = \frac{\left| s_{ii}^* s_{ij} + s_{ji}^* s_{jj} \right|^2}{\left(1 - \left(|s_{ii}|^2 + |s_{ji}|^2\right)\right) \left(1 - \left(|s_{jj}|^2 + |s_{ij}|^2\right)\right)} \tag{25}$$

with i and j are antenna's index number where $i \neq j$. These ECC show independency between antennas. If two antennas are completely independent, ECC value is 0. If these antennas are completely dependent, ECC value is 1. Requirement for diversity is set at ECC less than 0.5.
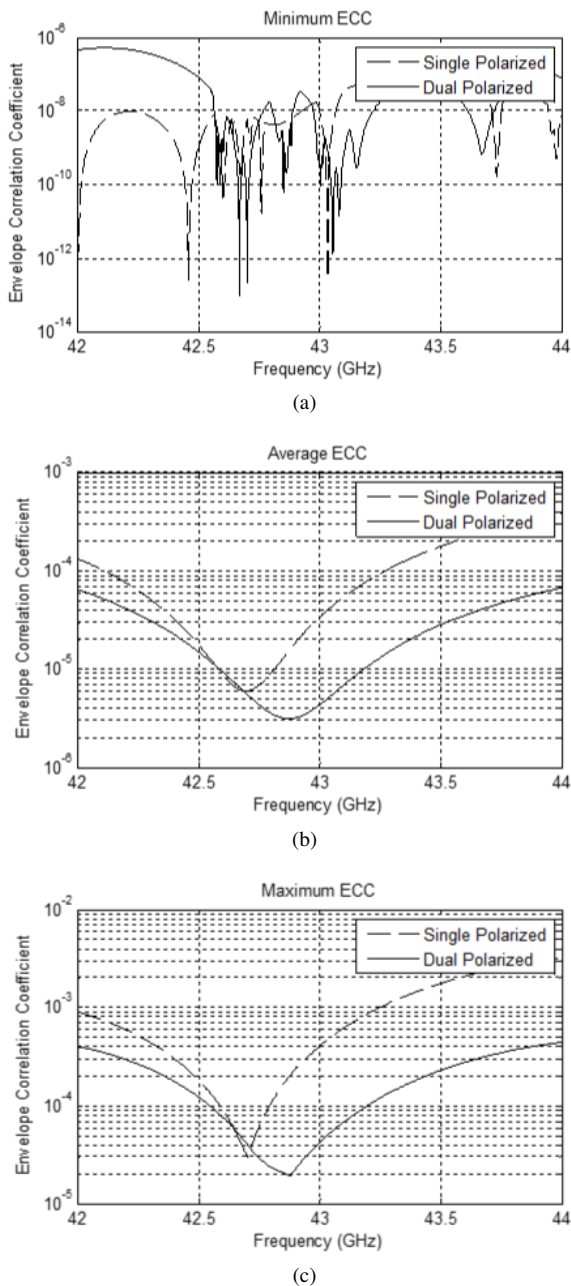
(a)

(b)

(c)

Fig. 7. Envelope correlation statistical value: (a) minimum, (b) average, (c) maximum
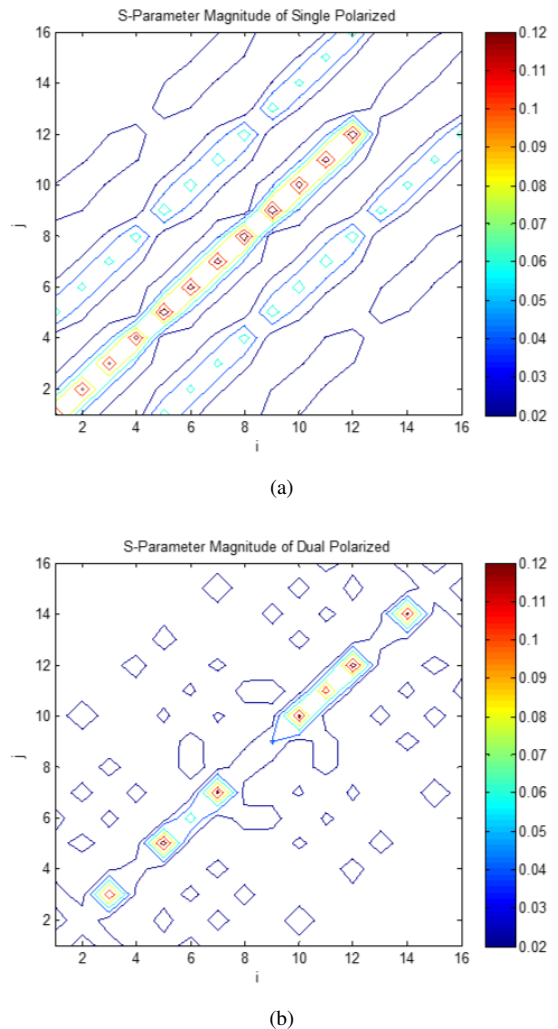

(a)

(b)

Fig. 8. Scattering parameter magnitude: (a) single polarized, (b) dual polarized.

Both of single polarized and dual polarized configurations has ECC lower than 0.5. It means diversity can be effectively applied on both configurations. Average ECC of both configurations are lower than 10^{-3} which is very small. Antennas correlation is neglected because of very low ECC.

There are two main focuses on lowering ECC. The most popular technique is by reducing coupling between antennas. This coupling is presented by $s_{ij} = s_{ji}$ with $i \neq j$. It mainly can be reached by making orthogonal radiation pattern or polarization. These orthogonality represents relation between related antennas. Designing low return loss antennas also can reduce correlation between antennas.

There are 120 pairs of ECC for 16 elements antenna. It is simplified to only presents minimum, average, and maximum value of ECC as representations. These statistical value contain range and mean of all ECC values. Fig. 7 shows minimum, average, and maximum value of ECC. Lower ECC is shown by dual polarized configuration. ECC value also has impact on diversity gain. This relation is presented in [21] by

$$G_{div} = 10\sqrt{1 - |\rho_{env}|}. \qquad (26)$$

Lower ECC means greater diversity gain at related pair of antennas. Dual polarized configuration also provides polarization diversity. Theoretically, dual polarized configuration has better performance on diversity compared to single polarized configuration.

A. Various α without Deviation

Dual polarized configuration has lower coupling compared to single polarized configuration as shown in Fig. 8. The highest coupling on single polarized and dual polarized configuration is -22.98 dB and -29.29 dB, respectively. The highest return loss on single polarized and dual polarized configuration is -17.18 dB and -17.58 dB, respectively. In this case, lower ECC on dual polarized configuration is more caused by lower
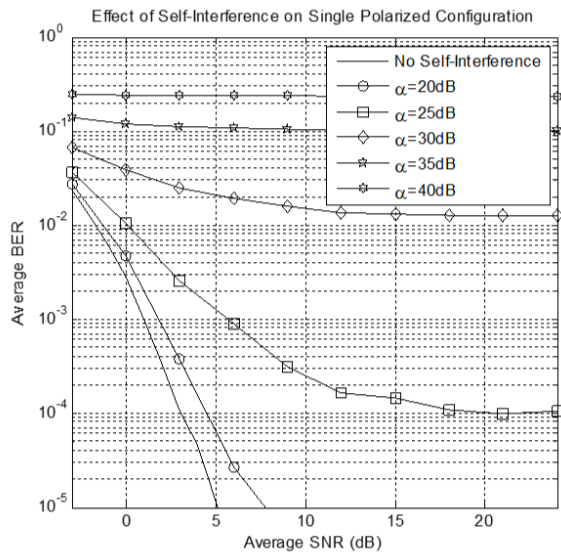
(a)
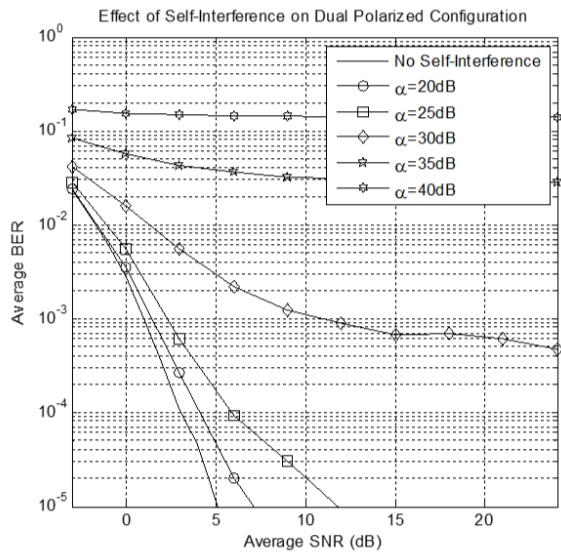
(b)

Fig. 9. System performance in various self-interference signal power ratio: (a) single polarized, (b) dual polarized.

coupling rather than lower return loss.

V. SYSTEM PERFORMANCE ON FULL DUPLEX SINGLE CHANNEL

System performances are tested on 16×16 MIMO configuration. Correlation between antennas are neglected because the values of ECC in center frequency are below 10^{-3}. Several self-interference signal power ratio is applied. Full rate QOSTBC with 16 antennas is applied with EVCM representation.

Both single polarized and dual polarized configurations are tested using S-parameter of antennas from antenna simulation. These values at magnitude representation are presented in Fig. 8. These values are used as in the systems simulation.
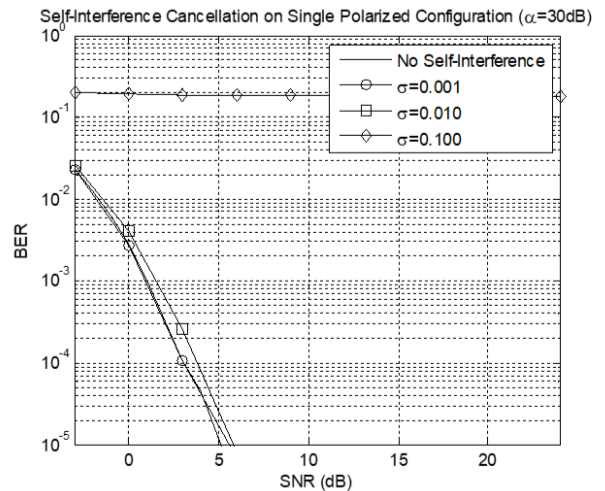
(a)
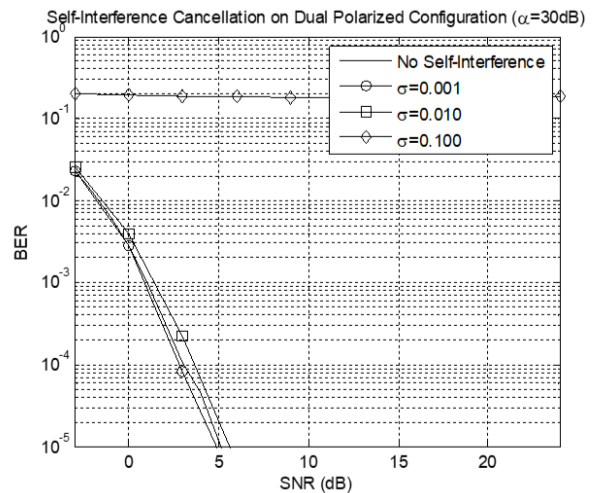
(b)

Fig. 10. System performance with $\alpha = 30$ dB with deviation and self-interference cancellation: (a) single polarized, (b) dual polarized.

Experiment results are classified into three categories: good, bad, and very bad. System is classified as good if there is no error floor in the simulation result. Bad classification is made for system with error floor. If total error or flat BER is happened, result is classified as very bad.

System performance of both single polarized and dual polarized configurations are shown in Fig. 9. It has been shown that dual polarized configuration has better performance than single polarized configuration. Lower BER at the same self-interference signal power ratio and SNR has been achieved by dual polarized configuration.

There is critical range at α of 20dB until 35dB for single polarized configuration and 25dB until 40dB for dual polarized configuration. Performance change drastically in critical range region from good to very bad. Critical range of dual polarized configuration is at the larger α compared to single polarized configuration. This critical range shows that dual polarized configuration has better stability by changing of α.

A. Deviated S-Parameter

Based on simulation result without deviation, $\alpha = 30\text{dB}$ is taken for simulation with deviated **S** because of its critical range. Both of single polarized and dual polarized are classified as bad in this research's classification.

Results of simulation with self-interference cancellation at $\alpha = 30$ dB are presented in Fig. 10. It has been shown that the result of single polarized and dual polarized configuration are relatively similar. It is because self-interference cancellation cancels the self-interference from other antennas. We also found that higher deviation of S-parameter leads to higher error because the deviation makes error on self-interference cancellation using basic (constant) S-parameter.

VI.   Conclusion

We have proposed dual-cross-polarized antenna decoupling for 43 GHz Planar Massive MIMO in Full Duplex Single Channel Communications. We designed dual-cross polarized antenna such that coupling between antennas can be reduced using different polarization for nearby antenna. The results confirmed that the proposed antenna reduces coupling by average of 37.83% at 43 GHz, reduces ECC by average of 89.69% at 43 GHz, and provide lower BER in self-interference environment compared to single polarized antenna configuration.

References

[1] E. Yaacoub, M. Husseini, and H. Ghaziri, "An overview of research topics and challenges for 5G massive MIMO antennas," in *2016 IEEE Middle East Conference on Antennas and Propagation (MECAP)*. IEEE, 2016, pp. 1–4.

[2] E. G. Larsson, O. Edfors, F. Tufvesson, and T. L. Marzetta, "Massive mimo for next generation wireless systems," *arXiv preprint arXiv:1304.6690*, 2013.

[3] L. Lu, G. Y. Li, A. L. Swindlehurst, A. Ashikhmin, and R. Zhang, "An overview of massive mimo: Benefits and challenges," *IEEE journal of selected topics in signal processing*, vol. 8, no. 5, pp. 742–758, 2014.

[4] J. I. Choi, M. Jain, K. Srinivasan, P. Levis, and S. Katti, "Achieving single channel, full duplex wireless communication," in *Proceedings of the sixteenth annual international conference on Mobile computing and networking*. ACM, 2010, pp. 1–12.

[5] S. Li and R. D. Murch, "An investigation into baseband techniques for single-channel full-duplex wireless communication systems," *IEEE Transactions on Wireless Communications*, vol. 13, no. 9, pp. 4794–4806, 2014.

[6] M. Jain, J. I. Choi, T. Kim, D. Bharadia, S. Seth, K. Srinivasan, P. Levis, S. Katti, and P. Sinha, "Practical, real-time, full duplex wireless," in *Proceedings of the 17th annual international conference on Mobile computing and networking*. ACM, 2011, pp. 301–312.

[7] Y. Hua, P. Liang, Y. Ma, A. C. Cirik, and Q. Gao, "A method for broadband full-duplex mimo radio," *IEEE Signal Processing Letters*, vol. 19, no. 12, pp. 793–796, 2012.

[8] C. Campolo, A. Molinaro, A. O. Berthet, and A. Vinel, "Full-duplex radios for vehicular communications," *IEEE Communications Magazine*, vol. 55, no. 6, pp. 182–189, 2017.

[9] Muhsin, R. P. Astuti, and B. S. Nugroho, "Dual polarized antenna decoupling for 60 GHz planar massive mimo," in *2017 International Conference on Signals and Systems (ICSigSys)*. IEEE, 2017, pp. 158–162.

[10] A. Alfakhri, M. A. Ashraf, A. Alasaad, and S. Alshebeili, "Design and analysis of compact size dual polarised ultra wideband MIMO antennas with simple decoupling structure," in *2016 21st International Conference on Microwave, Radar and Wireless Communications (MIKON)*. IEEE, 2016, pp. 1–4.

[11] M. M. M. Ali and A.-R. Sebak, "Design of compact millimeter wave massive MIMO dual-band (28/38 GHz) antenna array for future 5g communication systems," in *2016 17th International Symposium on Antenna Technology and Applied Electromagnetics (ANTEM)*. IEEE, 2016, pp. 1–2.

[12] A. Alfakhri, M. A. Ashraf, A. Alasaad, and S. Alshebeili, "A compact size ultra wideband MIMO antenna with simple decoupling structure," in *2016 17th International Symposium on Antenna Technology and Applied Electromagnetics (ANTEM)*. IEEE, 2016, pp. 1–2.

[13] Muhsin and K. Anwar, "Abba dual-cross-polarized antenna decoupling for 5g 16-element planar mimo at 28 ghz," in *2018 2nd International Conference on Telematics and Future Generation Networks (TAFGEN)*. IEEE, 2018, pp. 1–6.

[14] A. Sabharwal, P. Schniter, D. Guo, D. W. Bliss, S. Rangarajan, and R. Wichman, "In-band full-duplex wireless: Challenges and opportunities," *IEEE Journal on selected areas in communications*, vol. 32, no. 9, pp. 1637–1652, 2014.

[15] R. Garg, *Microstrip antenna design handbook*. Artech house, 2001.

[16] P. Meerasri, P. Uthansakul, and M. Uthansakul, "Self-interference cancellation-based mutual-coupling model for full-duplex single-channel mimo systems," *International Journal of Antennas and Propagation*, vol. 2014, 2014.

[17] H. Jafarkhani, "A quasi-orthogonal space-time block code," *IEEE Transactions on Communications*, vol. 49, no. 1, pp. 1–4, 2001.

[18] P. Marsch, W. Rave, and G. Fettweis, "Quasi-orthogonal stbc using stretched constellations for low detection complexity," in *2007 IEEE Wireless Communications and Networking Conference*. IEEE, 2007, pp. 757–761.

[19] A. A. Glazunov, "Mean effective gain of user equipment antennas in double directional channels," in *15th IEEE International Symposium on Personal, Indoor and Mobile Radio Communications (PIMRC) 2004*, vol. 1. IEEE, 2004, pp. 432–436.

[20] S. Blanch, J. Romeu, and I. Corbella, "Exact representation of antenna system diversity performance from input parameter description," *Electronics letters*, vol. 39, no. 9, pp. 705–707, 2003.

[21] S. K. Dhar and M. S. Sharawi, "A uwb semi-ring mimo antenna with isolation enhancement," *Microwave and Optical Technology Letters*, vol. 57, no. 8, pp. 1941–1946, 2015.